

Velocity Field Analysis of Bonding Interface on Cold-Rolled Copper/Aluminum Composite Plate

Huang Qingxue, Zhang Jiang, Zhu Lin, Jiang Li, Gao Xiangyu

Heavy Machinery Engineering Research Center of the Ministry of Education, Taiyuan University of Science and Technology, Taiyuan 030024, China

Abstract: The cold-rolled bonding process of copper/aluminum bimetal plate was investigated by the velocity field of finite element method (FEM). At the same time, deformation characteristics of metal were analyzed in the bonding process. The study method was to combine theory calculation with field data. The circumferential velocity of rollers, rolling reduction rate, synchronous rolling of non-equal sized rollers and asymmetrical rolling of non-equal sized rollers were analyzed. Results show that the velocity field can explain the cold-rolled bonding process of copper/aluminum bimetal plate more effectively; the synchronicity of metal flow on bonding surface decreases with the increase of circumferential velocity about rollers near the exit of deformation area, and the bonding strength is reduced; in the process of synchronous rolling about non-equal sized rollers, diameter ratio of the rolls is 1.4~1.6 with a great synchronicity of metal flow near the exit of deformation area and a high bonding strength; in the process of asymmetrical rolling about non-equal sized rollers, the circumferential velocity rate of rollers is 1.2 with a great synchronicity of metal flow near the exit of deformation area and a high bonding strength.

Key words: deformation characteristics; velocity field; bonding strength

Copper/aluminum bimetal plate is a new type of material with different mechanical, physical and chemical properties. It presents the relatively high electric and heat performance as copper, and exhibits the erosion-resistance, economy and light weight as aluminum, which is widely used in vehicles, aerospace, electronic appliances, energy and other fields^[1,2].

The influence of annealing-treatment on bonding interface structure and properties of copper/aluminum bimetal plate has been investigated by scholars in China^[3], and the roll-cladding technology for copper/aluminum sheet has been analyzed^[4,5]. The effect of rolling direction on the creep process of copper/aluminum bimetallic sheet^[6] and the process of accumulative roll bonding and folding have been researched by scholars^[7,8]. Studies mentioned above are to be carried out through experiment, but the cold-rolled bonding process of copper/aluminum bimetal plate is difficult to describe clearly with the complex deformation, and the influence of different craft parameters on bonding strength is hard to predict. So, a

new method is proposed, where the cold-rolled bonding process of copper/aluminum bimetal plate is investigated by the velocity field of finite element method (FEM). The deformation characteristics of copper/aluminum bimetal plate are analyzed in the cold-rolled bonding process. This paper took the integration of measures including numerical simulation and field tests, and the circumferential velocity of rolling, synchronous rolling of non-equal sized rollers and asymmetrical rolling of non-equal sized rollers were analyzed.

1 Velocity Field Principle of Slip-line Field

The ideal plastic flow theory of rigid plastic material is based on the following six assumptions in this paper:

(1) Copper plate and aluminum plate are assumed to be isotropic material, and the influence of oxide film on the surface of the plates is ignored in the cold-rolled bonding process.

(2) The rolls are assumed to be rigid body without deformation in the cold-rolled bonding process.

Received date: July 14, 2016

Foundation item: National Key Basic Research Development Program of China ("973" Program) (2012CB722801)

Corresponding author: Huang Qingxue Ph. D., Professor, Heavy Machinery Engineering Research Center of the Ministry of Education, Taiyuan University of Science and Technology, Taiyuan 030024, P. R. China, E-mail: hqx@tyust.edu.cn

Copyright © 2017, Northwest Institute for Nonferrous Metal Research. Published by Elsevier BV. All rights reserved.

(3) Copper plate and aluminum plate are assumed to be without any defects, and the influences of micro cracks or voids of the microstructure are ignored in the cold-rolled bonding process.

(4) In the cold-rolled bonding process, the volume of plates is a constant:

$$d\varepsilon_x + d\varepsilon_y + d\varepsilon_z = d\varepsilon_1 + d\varepsilon_2 + d\varepsilon_3 = 0$$

(5) At each load moment, the principal axes of stress and the principal axes of strain increment coincide.

(6) In plastic mechanics, the material meets the standard Mises yield criterion^[9]:

$$J_2 - k^2 = 0 \tag{1}$$

where, J_2 is the second invariant of deviator stress tensor, and k is the material yield strength under the pure shear state.

According to the Levy-Mises plastic flow rule of ideal rigid-plastic material^[9]:

$$d\varepsilon_{ij} = \sigma_{ij}' d\lambda \tag{2}$$

where, ε_{ij} is the strain tensor, σ_{ij} is the stress partial tensor, and $d\lambda$ is positive instantaneous constant.

Eq.(2) is divided by the dt of the time increment on both sides, and the stress-strain rate equation^[10] is concluded:

$$\dot{\varepsilon}_{ij} = \dot{\sigma}_{ij}' \tag{3}$$

where, $\dot{\varepsilon}_{ij} = \frac{d\varepsilon_{ij}}{dt}$ and $\dot{\sigma}_{ij}' = \frac{d\sigma_{ij}'}{dt}$.

According to Eq.(3), the stress-strain rate equations^[10] is obtained under the plane strain state:

$$\begin{aligned} \dot{\varepsilon}_x &= \dot{\sigma}_x' = \dot{\sigma}_x - \sigma_m \dot{\gamma} \\ \dot{\varepsilon}_y &= \dot{\sigma}_y' = \dot{\sigma}_y - \sigma_m \dot{\gamma} \\ \dot{\varepsilon}_{xy} &= \dot{\sigma}_{xy}' = \dot{\sigma}_{xy} \end{aligned} \tag{4}$$

The point (x, y) of Eq.(4) is transferred to the coordinate system of slip line about α and β , in Eq.(4) where $\sigma_x = \sigma_\alpha$, $\sigma_y = \sigma_\beta$, $\dot{\varepsilon}_x = \dot{\varepsilon}_\alpha$ and $\dot{\varepsilon}_y = \dot{\varepsilon}_\beta$.

σ_α and σ_β are the normal stresses on the plane where the maximum shear stress is to be. So, according to plane strain characters in plasticity, the relation is expressed by the following equation:

$$\sigma_\alpha = \sigma_\beta = \sigma_m \tag{5}$$

where σ_m is the average stress.

Eq.(5) is plugged into Eq.(4), and the relations can be described by the following equation:

$$\begin{aligned} \dot{\varepsilon}_\alpha &= \frac{d\varepsilon_\alpha}{dt} = 0 \\ \dot{\varepsilon}_\beta &= \frac{d\varepsilon_\beta}{dt} = 0 \end{aligned} \tag{6}$$

Eq.(6) can show that slip line is to be without strain increment, in other words, the slip line does not have the scalable characteristic^[9].

As shown in Fig.1, we can assume that there are two points P_1 and P_2 , which are infinitely close to each other on the slip line. The speed is v_1 at location P_1 and the speed is v_2 at location P_2 . The velocity components of v_1 are v_α and v_β ,

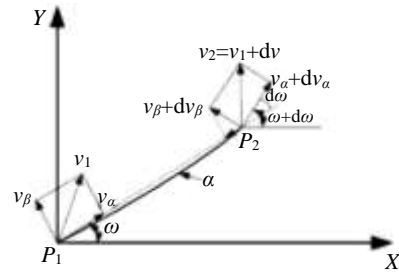


Fig.1 Decomposition of speed about two points on the slip line

along the slip line directions. The velocity components of v_2 are $v_\alpha + dv_\alpha$ and $v_\beta + dv_\beta$, respectively, along the slip line directions. The angle is $d\omega$ from P_1 to P_2 . Because P_1 is infinitely close to P_2 , we can think $\overline{P_1P_2}$ overlaps with $\overline{P_1P_2}$. According to the not scalable characteristic of the slip line, we can realize that the velocity components of P_1 and P_2 are equal, on the direction of $\overline{P_1P_2}$ and on the direction which is perpendicular to $\overline{P_1P_2}$. The relations can be described by the following equations:

$$\begin{aligned} v_\alpha &= v_\alpha + dv_\alpha \cos d\omega \\ v_\beta &= v_\beta + dv_\beta \sin d\omega \\ v_\beta &= v_\beta + dv_\beta \cos d\omega \\ v_\alpha &= v_\alpha + dv_\alpha \sin d\omega \end{aligned} \tag{7}$$

because the $d\omega$ is a very small value, these formulas are valid in Eq.(7): $\cos d\omega \gg 1$, $\sin d\omega \gg d\omega$; at the same time, $dv_\beta \sin d\omega$ and $dv_\alpha \sin d\omega$ can be ignored. Eq.(7) can be described by the following equation:

$$\begin{aligned} dv_\alpha - v_\beta d\omega &= 0 \\ dv_\beta + v_\alpha d\omega &= 0 \end{aligned} \tag{8}$$

Eq.(8) can be described by the corresponding difference equation:

$$\begin{aligned} v_\beta &= \frac{Dv_\alpha}{D\omega} \\ v_\alpha &= -\frac{Dv_\beta}{D\omega} \end{aligned} \tag{9}$$

It can be shown very easily from Eq.(9) that if v_α and v_β are known and the angle ω has an increment of $D\omega$, the velocity values about $v_{\alpha1}$ and $v_{\beta1}$ of the next point on the slip line can be obtained.

At this point, the velocity of grid-point can be given by the following equation:

$$v = v_{\alpha1} + v_{\beta1} \tag{10}$$

2 Velocity Field Analysis of Cold-rolled Bonding Process

2.1 Building model

The cold-rolled bonding process of copper/aluminum bimetal plate is a typical problem of material non-linearity,

geometric non-linearity and boundary condition non-linearity. So, the C3D8R element was used for meshing the frame of Cu/Al plates in this model, which would reduce the hourglass phenomenon and decrease computation time.

The cold-rolled bonding process is a severe deformation problem. In order to bite successfully, the copper/aluminum bimetal plate had two grooves about 30°. In a steel plant, the combined slab was 1500 mm in length and 200 mm in width, and the thickness of the copper plate and aluminum plate were 3 and 5 mm, respectively. In order to save computation time, the combined slab was 60 mm in length and 50 mm in width. The longitudinal size of the combined slab is shown in Fig.2. Finally, the copper plate was divided into 2706 units and 4284 nodes and the aluminum plate was divided into 4059 units and 5712 nodes.

In the model, the properties of material used are shown in the Table 1.

2.2 Boundary conditions

The center coordinates were defined on the center of the upper and lower rolls.

Two pairs of contact surface were set up, where the copper plate was contacted with the upper roll and the aluminum plate was contacted the with lower roll. The angular velocity of upper and lower rollers is defined by the following equations:

$$\begin{aligned} \omega_{y1}|_{t=0} &= A \begin{matrix} \ddot{y} \\ \ddot{z} \\ \ddot{x} \end{matrix} \\ \omega_{x1}|_{t=0} &= \omega_{z1}|_{t=0} = 0 \end{aligned} \quad (11)$$

$$\begin{aligned} \omega_{y2}|_{t=0} &= B \begin{matrix} \ddot{y} \\ \ddot{z} \\ \ddot{x} \end{matrix} \\ \omega_{x2}|_{t=0} &= \omega_{z2}|_{t=0} = 0 \end{aligned} \quad (12)$$

where A and B are constants, which are given by different process.

A pair of contact surface was set up, where the aluminum plate was contacted with the copper plate. The initial velocity of the copper and aluminum plate is defined by the following equations:

$$\begin{aligned} v_{x1}|_{t=0} &= -50 \text{ mm/s} \begin{matrix} \ddot{y} \\ \ddot{z} \\ \ddot{x} \end{matrix} \\ v_{y1}|_{t=0} &= v_{z1}|_{t=0} = 0 \end{aligned} \quad (13)$$

$$\begin{aligned} v_{x2}|_{t=0} &= -50 \text{ mm/s} \begin{matrix} \ddot{y} \\ \ddot{z} \\ \ddot{x} \end{matrix} \\ v_{y2}|_{t=0} &= v_{z2}|_{t=0} = 0 \end{aligned} \quad (14)$$

In the model, the interaction of sliding surfaces is modeled with a Coulomb friction law:

$$\tau = \mu \sigma_n \quad (15)$$

where τ is the friction shear stress, σ_n is the normal pressure stresses on the shear plane, and μ is the friction coefficient. The friction coefficient between upper roll and copper plate is 0.15, that between lower roll and aluminum plate is 0.2, and that between copper plate and aluminum plate is 0.2.

3 Results and Discussion

3.1 Velocity field model analysis

The velocity model of cold-rolled bonding process about copper/aluminum bimetal plate is shown in Fig.3. Fig.4 is a drawing of partial enlargement for A in Fig.3. In the model, the rolling reduction rate was 70%, the working roll diameters were both $\Phi 320$ mm, the roll length were both 350 mm, and the angular velocity were both 0.75 rad/s, as circumferential velocity about rollers being 120 mm/s.

According to the deformation characteristics in the cold-rolled bonding process, the deformation area can be divided into four parts, as shown in Fig.3. Part I: the elastic deformation of copper/aluminum plate is displayed at the bite stage. Part II: the elastic deformation of copper plate and the plastic deformation of aluminum plate are displayed. Part III: with the increase of deformation, the remarkable work hardening is caused about aluminum plate, which forces the plastic deformation of copper plate. Part IV: with the increase of copper/aluminum plate's plastic deformation, working hardening occurs in aluminum plate and copper plate.

As shown in Fig.3 and Fig.4, in the part I, II, III and IV, the speed of the corresponding nodes are different on the contact surfaces of copper/aluminum plate, and the values of differences decrease gradually in the cold-rolled bonding process. At the exit of work piece, the speed of the corresponding nodes across the width is shown in Fig.5, and it's basically identical. So, we can consider that the contact surfaces have been bonding.

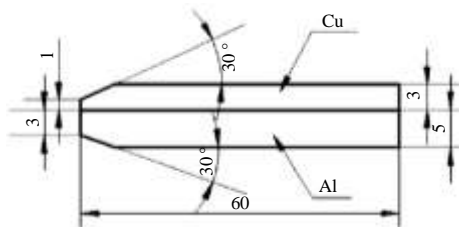


Fig.2 Longitudinal size of slab

Table 1 Properties of materials

Material	E/GPa	$\rho/g \text{ cm}^{-3}$	ν	σ_s/MPa	Tangent modulus/MPa
Cu	108	8.5	0.325	33.3	465
Al	68	2.702	0.34	20	138

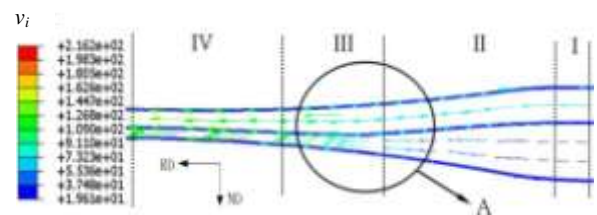


Fig.3 Model of velocity field

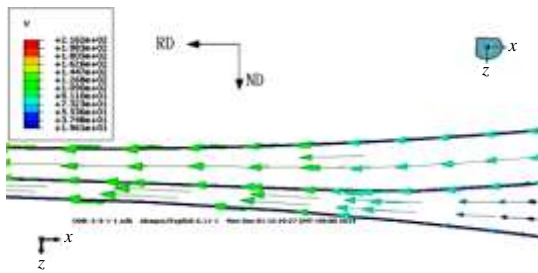


Fig.4 Drawing of partial enlargement about A in Fig.3

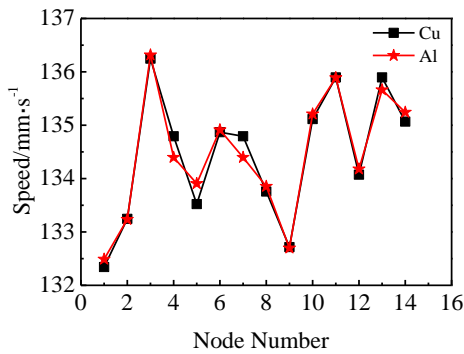


Fig.5 Speed of corresponding node across the width

3.2 Rolling velocity analysis

In the model, the diameters of working rolls were $\Phi 320$ mm, the length was 350 mm, and the rolling reduction rate was 70%. The values of circumferential velocity of working rolls were 120, 200, 280, 500, 750 and 1000 mm/s. The influences on cold-rolled bonding process were analyzed for

different circumferential velocities about working rolls.

Under the six-group different circumferential rolling velocities, the speed distribution of the corresponding nodes on composite surfaces is shown in Fig. 6. The speed is unstable, as the composite plate first enters the deformation area. Under these five statuses of Fig. 6a–6e, the values of speed tend to accord with each other, as the composite plate is out of the deformation area. Under the state of Fig.6f, the values of speed are inconsistent in the whole deformation area. The synchronicity of speed decreases with the increase of rolling velocity near the exit of deformation area. In a steel plant, the six-group bimetal plates after cold rolling were annealed. The annealing temperature was 350 °C with holding for 30 min followed by going down to room temperature. The corresponding peel strength is shown in Fig.7, and the values decrease with the increase of rolling velocity.

Through the above comparative analysis, we may draw such conclusions: As the composite plate first enters the deformation area, the speed of contact surfaces is unstable, which results in different degrees of asymmetrical rolling. The synchronicity of metal flow on bonding surface decreases with the increase of rolling velocity near the exit of deformation area. The bonding strength decreases with the increase of rolling velocity. Because the bonding strength can't meet the demand of the practice, as the rolling velocity is greater than 750 mm/s. Therefore, the circumferential rolling velocity is less than 750 mm/s.

3.3 Synchronous rolling of unequal sized rollers analysis

In the model, the length of working rolls were 350 mm, the value of circumferential velocity of working rolls was 120 mm/s and the rolling reduction rate was 65%. The diameters of

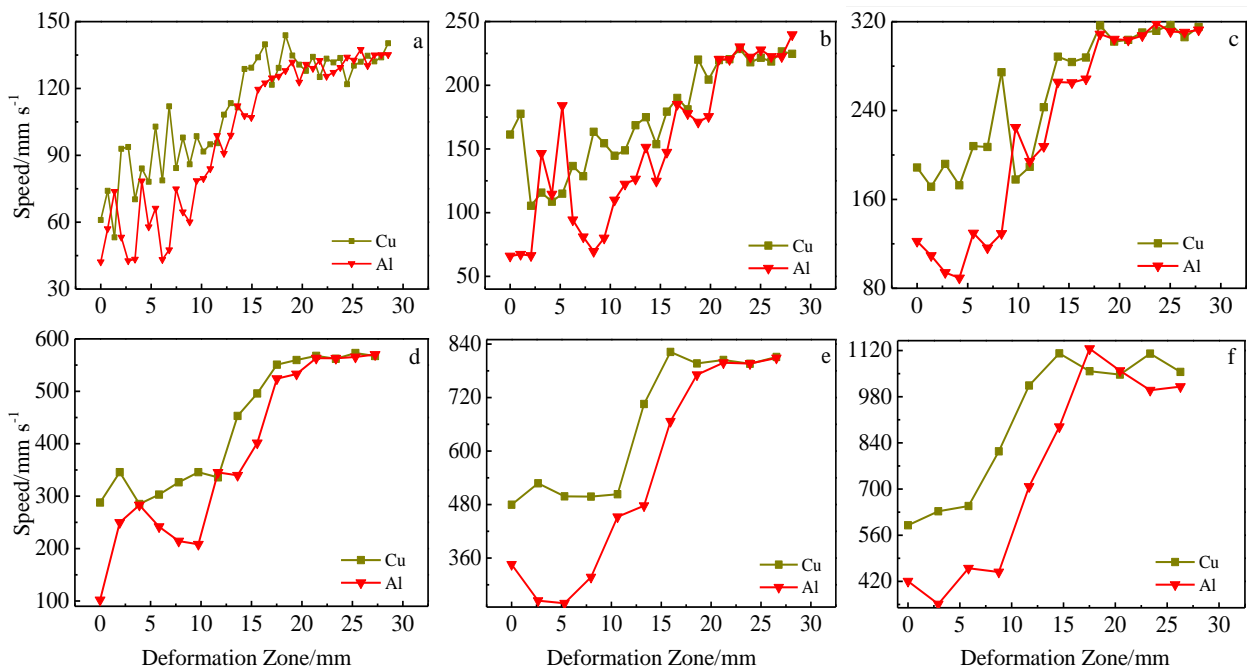


Fig. 6 Velocity distribution of corresponding node on the composite surface under different rolling velocities: (a) 120 mm/s, (b) 200 mm/s, (c) 280 mm/s, (d) 500 mm/s, (e) 750 mm/s, and (f) 1000 mm/s

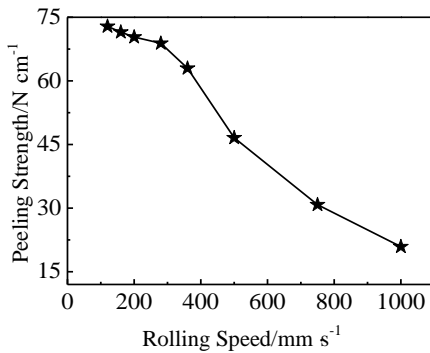


Fig.7 Distribution of peel strength under different circumferential velocity of working rolls

lower roll near the aluminum plate and upper roll near the copper plate are D_1 and D_2 , while the corresponding angular velocity is ω_1 and ω_2 , as shown in Table 2. The influences on cold-rolled bonding process were analyzed for different diameter ratio (D_1/D_2).

Under the five-group different diameter ratios, the speed distribution of the corresponding nodes on composite surfaces is shown in Fig.8. The synchronicity of speed is enhanced with the increase of diameter ratio near the exit of deformation area. The stability of speed is abated near the exit of deformation area, when the diameter ratio is larger than 1.6. In a steel plant, the five-group copper/aluminum bimetal plates after cold rolling were annealed. The annealing temperature was 350 °C with holding for 30 min followed by going down to room temperature. The corresponding peel strength is shown in Fig.9.

The values of peel strength increase firstly and then decrease slightly with the increase of diameter ratio. The values of peel strength are larger, when the diameter ratio is 1.4~1.6.

Through the above comparative analysis, we may draw such conclusions: The synchronicity of metal flow on bonding surfaces is enhanced with the increase of diameter ratio near the exit of deformation area. At the same time, the values of bonding strength increase firstly and then decrease slightly. The stability of speed about the corresponding nodes is abated to decrease slightly bonding strength, when the diameter ratio is larger than 1.6. Therefore, the diameter ratio (D_1/D_2) is 1.4~1.6.

3.4 Asymmetrical rolling of non-equal sized rollers analysis

In the model, the length of working rolls was 350 mm, the diameters of upper roll near the copper plate and lower roll near the aluminum plate were $\Phi 200$ mm and $\Phi 320$ mm respectively, and the rolling reduction rate was 65%. The circumferential velocity about upper roll and lower roll is v_1 and v_2 , while the corresponding angular velocity is ω_1 and ω_2 , as shown in Table 3. Under different diameters, the influences on cold-rolled bonding process were analyzed for different circumferential velocity rates of working rolls (v_1/v_2).

Under the four-group different circumferential velocity rate,

Table 2 Parameters of rollers

D_1 /mm	D_2 /mm	D_1/D_2	ω_1 /rad s ⁻¹	ω_2 /rad s ⁻¹
320		1	0.75	
384		1.2	0.625	
448	320	1.4	0.5357	0.75
512		1.6	0.4688	
640		2	0.375	

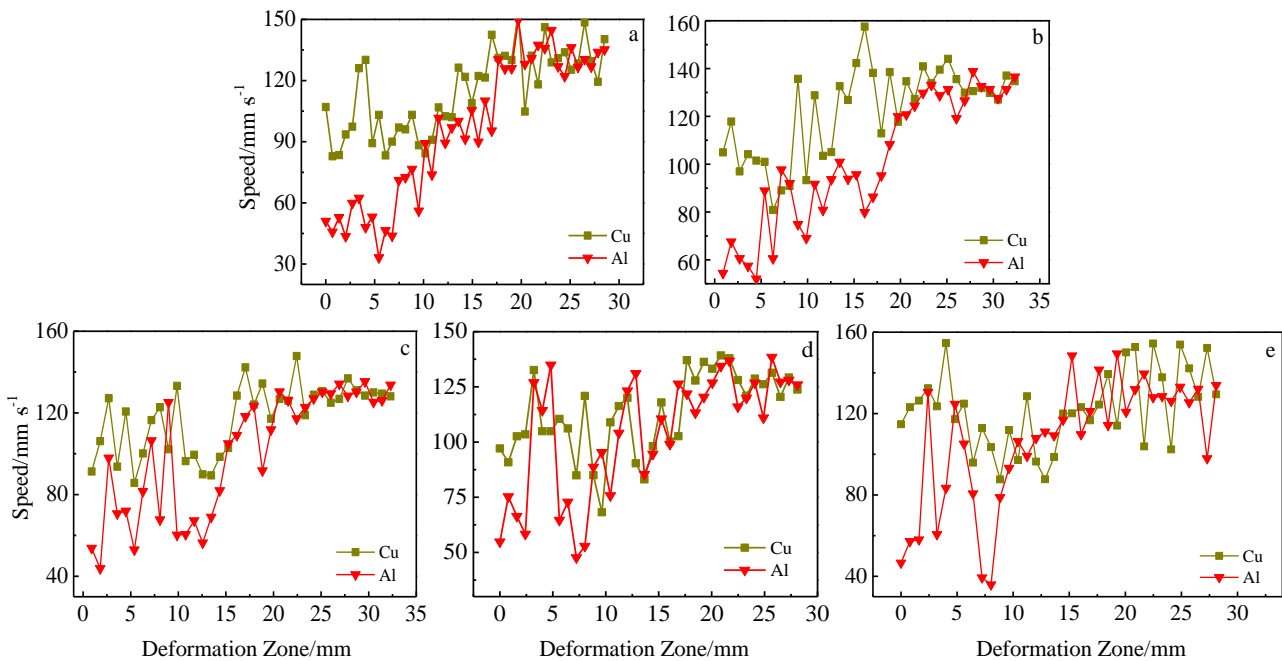


Fig.8 Velocity distribution of corresponding node on the composite surface under different diameter ratios (D_1/D_2): (a) 1, (b) 1.2, (c) 1.4, (d) 1.6, and (e) 2

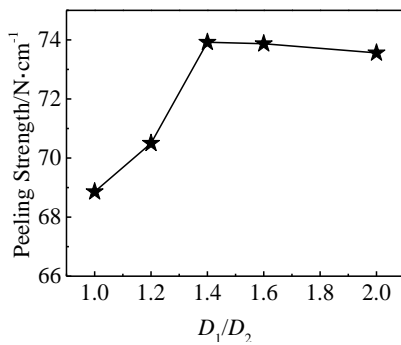


Fig. 9 Distribution of peel strength under different diameter ratios

the speed distribution of the corresponding nodes on composite surfaces is shown in Fig.10 about copper/aluminum bimetal plates. The synchronicity of speed is enhanced firstly and then decreases slightly with the increase of circumferential velocity rate near the outlet of deformation area. When the

circumferential velocity rate is 1.2, the synchronicity of speed is the best near the exit of deformation area. The stability of speed is abated near the exit of deformation area, when the circumferential velocity rate is larger than 1.4. In a steel plant, the four-group copper/aluminum bimetal plates after cold rolling were annealed. The annealing temperature was 350 °C with holding for 30 min and then went down to room temperature. The corresponding peel strength is shown in Fig.11. The values of peel strength increase firstly and then decrease slightly with the increase of circumferential velocity rate about rollers, and the value is the largest, when the circumferential velocity rate is 1.2.

Table 3 Parameters of rollers

$\omega_1/rad\ s^{-1}$	$v_1/mm\ s^{-1}$	$\omega_2/rad\ s^{-1}$	$v_2/mm\ s^{-1}$	v_1/v_2
1.6	120			1
1.92	144	0.75	120	1.2
2.24	168			1.4
2.56	192			1.6

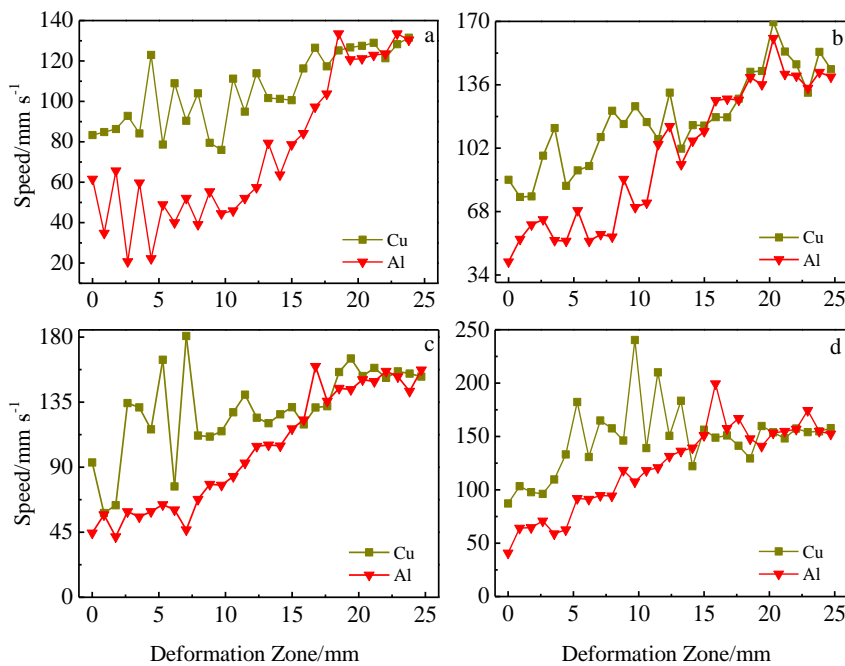


Fig.10 Velocity distribution of corresponding node on the composite surface under different velocity rates v_1/v_2 : (a) 1, (b) 1.2, (c) 1.4, and (d) 1.6

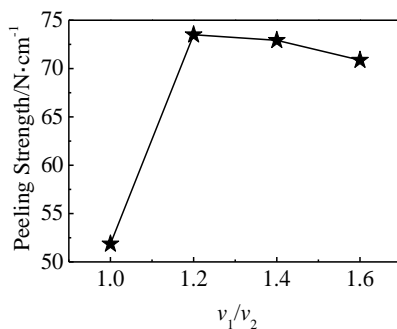


Fig.11 Distribution of peel strength under different circumferential velocity rates of rolling

Through the above comparative analysis, we may draw such conclusions: The synchronicity of metal flow on bonding surface is enhanced firstly and then diminished with the increase of circumferential velocity rate near the exit of deformation area. At the same time, the values of bonding strength increase firstly and then decrease slightly. The stability of speed about the corresponding nodes is abated to decrease slightly bonding strength, when the circumferential velocity rate is larger than 1.2. Therefore, the circumferential velocity rate (v_1/v_2) is 1.2.

4 Conclusions

1) The velocity field can explain the cold-rolled bonding process of copper/aluminum bimetal plate more effectively.

2) The synchronicity of metal flow on bonding surface decreases with the increase of circumferential velocity near the exit of deformation area and the bonding strength decreases too. The circumferential velocity of rollers is less than 750 mm/s.

3) In the bonding process of synchronous rolling with non-equal sized rollers, the synchronicity of metal flow on bonding surface is enhanced with the increase of diameter ratio near the exit of deformation area. At the same time, the bonding strength increases firstly and then decreases slightly, and the rolling force increases gradually. The stability of speed about the corresponding nodes is abated to decrease slightly bonding strength, when the diameter ratio is larger than 1.6. Therefore, the diameter ratio is 1.4~1.6.

4) In the bonding process of asymmetrical rolling with non-equal sized rollers, the synchronicity of metal flow on bonding surface is enhanced firstly and then diminished with the increase of circumferential velocity rate near the exit of deformation area. At the same time, the bonding strength increases firstly and then decreases slightly, and the rolling force decreases gradually. The stability of speed is abated to

decrease slightly bonding strength, when the circumferential velocity rate is larger than 1.2. Therefore, the circumferential velocity rate (v_1/v_2) is 1.2.

References

- 1 Yang Y S, Yang D D. *Material & Heat Treatment*[J], 2011, 40(12): 107 (in Chinese)
- 2 Kwang S L, Yong-Nam K. *Transactions of Nonferrous Metals Society of China*[J], 2013, 23: 341
- 3 Lu W K, Xie J P, Wang A Q et al. *Special Casting & Nonferrous Alloys*[J], 2014, 34(2): 198 (in Chinese)
- 4 Huang H J, Zhang W Z, Wang S S et al. *Journal of Shenyang University of Technology*[J], 2009, 31(5): 531 (in Chinese)
- 5 Yu Y, Song H W, Chen Y et al. *Materials Science and Technology* [J], 2014, 22(5): 13 (in Chinese)
- 6 Robert U. *Materials and Design*[J], 2013, 49: 693
- 7 Nagaraj V G, Jan G F, Bjørn H. *Materials and Design*[J], 2013, 52: 905
- 8 Mohammad R T, Roohollah J, Jan D et al. *Materials and Design* [J], 2013, 51: 274
- 9 Yu H Q, Chen J D. *Fundamental of Metal Plastic Forming*[M]. Beijing: China Machine Press, 2010: 107 (in Chinese)

冷轧铜铝复合板结合界面速度场分析

黄庆学, 张 将, 朱 琳, 蒋 莉, 高翔宇

(太原科技大学 重型机械教育部工程研究中心, 山西 太原 030024)

摘要: 通过有限 (FEM) 元速度场研究了冷轧铜铝双层板的复合过程, 将该过程中金属的变形特征进行了分析, 同时, 将有限元计算结果与某工厂数据相结合, 分析了轧制速度、压下率、异径同步、异径异步对铜铝双层板复合的影响。结果表明, 速度场模型能够更有效地说明铜铝板的复合过程; 轧制速度越大, 变形区出口处复合面金属流动的同步性越差, 复合强度越低; 异径同步轧制铜铝复合板时, 辊径比取 1.4~1.6, 变形区出口处复合面金属流动的同步性越好, 复合强度较高; 异径异步轧制铜铝复合板时, 轧制速比取 1.2, 变形区出口处复合面金属流动的同步性越好, 复合强度较高。

关键词: 变形特征; 速度场; 复合强度

作者简介: 黄庆学, 男, 1960 年生, 博士, 教授, 太原科技大学重型机械教育部工程研究中心, 山西 太原 030024, E-mail: hqx@tyust.edu.cn